International Journal of Modern Manufacturing Technologies
ISSN 2067–3604, Vol. XV, No. 2 / 2023
https://doi.org/ 10.54684/ijmmt.2023.15.2.56

INFLUENCE OF SUBSTRATE SURFACE ROUGHNESS ON PUSH-OFF STRENGTH FOR FRICTION SURFACING OF LOW CARBON STEEL WITH AA6061-T6 ALUMINIUM ALLOY

Gautam Chudasama[1], Sachin Wanare[2], Vivek Kalyankar[1]

[1]Advanced Welding Laboratory, Department of Mechanical Engineering, Sardar Vallabhbhai National Institute of Technology, Surat, Gujarat, India 395007
[2] Department of Mechanical Engineering, Dr. D.Y.Patil Institute of Engineering, Management and Research, Pune, Maharashtra, India, 411044

Corresponding author: Gautam Chudasama, gautamchudasama16@gmail.com

Abstract: Surface roughness plays an essential role in friction surfacing deposition as a smooth substrate surface polishes both consumable and substrate tools, resulting in a lack of deposition. Hence, an attempt is made to investigate the effect of substrate surface roughness while friction surfacing of AA6061-T6 coating on CR01 low carbon steel and its performance is compared through push-off strength. It is revealed that with an increase in substrate surface roughness, more rubbing action occurs between consumable tool and substrate, which results in higher heat generation and reduction in deposition thickness. The grain refinement is observed at the coating region due to dynamic recrystallisation, which results in fine grain microstructure. The substrate with R_a roughness values 1.5-2.5, 5.5-6.5 and 7.5-8.5 µm showed 26, 32 and 45 MPa push-off strength, respectively. Hence, it is inferred that the push-off strength increases substantially with an increase in the substrate surface roughness.
Keywords: AA6061, CR01 low carbon steel, Friction surfacing, Substrate surface roughness, Push-off strength

1. INTRODUCTION

Friction surfacing is a solid-phase material bonding process used to provide specific properties to the substrate material by the deposition of superficial material on its surface. The process involves plastic deformation of a rotating metallic consumable tool, which is forced against the substrate material with applied axial load, as presented in Fig. 1. The relative motion between the consumable tool and substrate generates friction heat and results in the formation of the solid phase metallurgical bond between plasticised material and substrate due to the interdiffusion across the interface. The friction surfacing process has several advantages over other deposition techniques, such as comparatively smaller heat-affected zone, lower residual stresses, absence of dilution, solidification shrinkage, etc. Since the process does not involve the melting of base metal, it can be applicable for dissimilar joining of materials such as steel, aluminium, magnesium, copper, nickel, etc., that are incompatible with liquid state processes [1]. The most influencing friction surfacing process parameters are spindle speed, axial force and table travel speed [1,2].

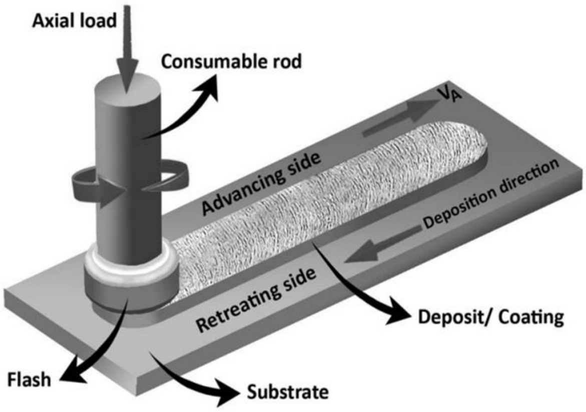

Fig. 1. Schematic diagram of friction surfacing process [3]

Kumar et al. [4] examined the effect of axial force, spindle speed and table speed on bonding strength and bend ductility for the deposition of AA6063 on the mild steel surface. The authors concluded that 1.25-1.3 mm deposition thickness provides maximum strength and ductility. Kallien et al. [5] investigated the effect of process temperature on deposition geometry for friction surfacing of AA 5083 H112 on AA 7050 T7451. Spindle speed and axial force are dominant process parameters affecting temperature during deposition. The higher temperature provides thinner and wider deposition [5].

Vitanov et al. [6] demonstrated that friction surfacing deposition can be possible on non-specialised equipment such as a machining centre. Authors varied spindle speed, consumable tool feed rate and table travel to investigate the performance instead of spindle speed, axial force and table travel speed. Moreover, Galvis et al. [7] and Da silva et al. [8] investigated the suitability of friction surfacing on conventional milling machine and vertical milling set-up, respectively. Additionally, Troysi et al. [9] concluded that a 0.5 ratio between the consumable tool feed rate and table travel speed provides good bonding for the deposition of stainless steel on low carbon steel.

Troysi et al. [10] concluded that although coating geometry does not have a significant impact of surface roughness, however adhesion between substrate and coating is largely affected by substrate surface roughness. Da Silva et al. [8] reported that the surface roughness of substrate material has significant impact on the push-off strength. It is also reported that the poor substrate surface roughness leads to limited adhesion between the substrate and the consumable rod, which leads to the dissipation of frictional heat through the consumable rod and the deposition of coating cannot be achieved. From the available literature, it is inferred that the surface roughness of substrate material has a significant impact on the deposition characteristics. However, the literature on the influence of substrate surface roughness on the push-off strength is scarce. In addition, thorough investigations related to the influence of substrate surface roughness would be beneficial to analyse the heat generation during the friction surfacing process, which would be useful to understand the behaviour of the substrate and coating materials under consideration.

In this article, efforts are made to examine the influence of the surface roughness of substrate material CR01 low carbon steel (LCS) on the deposition characteristics of the as-deposited AA6061-T6. The mechanical characterisation is performed by examining the push-off strength along with its microstructural characterisation. In this article, efforts are made to examine the influence of the surface roughness of substrate material on the deposition characteristics. The consumable tool made up of AA6061-T6 is used to deposit on the CR01 low carbon steel (LCS). The mechanical characterisation is performed by examining the push-off strength along with its microstructural characterisation.

2. EXPERIMENTAL APPROACH

A 2 mm thick CR01 LCS and 20 mm diameter AA6061-T6 rod are selected as substrate and consumable tool materials, respectively. Hereafter, AA6061-T6 deposition material refers to Al and substrate CR01 as steel for simplicity. The chemical compositions of both materials are presented in Table 1. The steel sheet is cut into (100 x 150)mm size, and the consumable rod is cut into the size of 200 mm long by considering the bucking of rod and set-up requirement. The face of the consumable rod is prepared by turning before the deposition to ensure a flat surface in order to improve contact with the substrate.

In order to examine the effect of substrate surface roughness, three different roughness values, as mentioned in Table 2, are produced on the steel surface with the help of different grits of sanding belts. Other important process parameters, such as spindle speed and table travel speed, are selected based on the previous research work and trial experiments. Consumable tool feed rate is taken as half of the table travel speed in order to provide good adhesion property between substrate and coating [8]. Fig. 2 shows the friction surfacing deposition sample for R_a between (7.5-8.5)µm steel surface roughness.

Table 1. The chemical composition of the substrate and tool materials

Material	C, [%]	Si, [%]	Mn, [%]	Mg, [%]	Al, [%]	Fe, [%]
AA6061-T6	-	0.62	0.09	1.19	Bal	0.172
CR01 (LCS)	0.06	0.01	0.16	-	0.049	Balance

Table 2. The friction surfacing process parameters

Sr. No.	Substrate surface roughness, R_a, [μm]	Other friction surfacing process parameters
1	1.5-2.5	Spindle speed: 1400 rpm Table speed: 200 mm/min Tool feed rate: 0.5 of table
2	5.5-6.5	Spindle speed: 1400 rpm Table travel speed: 200 mm/min Tool feed rate: 0.5 of table travel
3	7.5-8.5	Spindle speed: 1400 rpm Table travel speed: 200 mm/min Tool feed rate: 0.5 of table travel

Fig. 2. Friction surfacing deposited sample

Fig. 3. (a) Schematic diagram (b) actual image of the push-off test specimen and (c) fixture arrangement on universal tensile testing set-up

The bonding strength between substrate and deposited layer is investigated by the push-off test. The push-off test is carried out on the universal tensile testing machine (Make: Star testing system). Fig. 3 shows the schematic diagram, actual image of push-off test specimen and fixture arrangement on universal tensile testing set-up to evaluate the push-off strength. In addition to this, fractography of fractured sample is carried out by Field-emission-scanning electron microscopy (FE-SEM) (Make: Jeol).

Samples for metallurgical examinations are prepared by following standard metallurgical procedures. A Nital solution (96 ml ethanol and 4 ml HNO_3) and Keller's reagent (2.5 ml HNO_3, 1.5 ml HCL, 1 ml HF and 95 ml distilled water) are used for etching the steel and Al, respectively [11]. The macrostructure and microstructure of the as-deposited samples are examined by optical microscopy (Make: Leica Microsystem) and FE-SEM coupled with energy dispersive spectroscopy (EDS) analysis (Make: Jeol). Further, microhardness analysis is performed on Vicker's microhardness equipment (Make: Chennai Metco) with a load of 200 gm and a dwell time of 10 seconds.

3. RESULTS AND DISCUSSIONS

The performance of friction surfacing deposition is evaluated based on deposition morphology, metallurgical characterisation of coating and interface, mechanical characterisation, including push-off strength as well as fractography. Results for the same are summarised in the following subsections.

3.1. Deposition morphology

Fig. 4 shows the deposition morphology at different values of steel surface roughness, which indicates that uniform deposition without any major defects is possible by the selected combinations of process parameters.

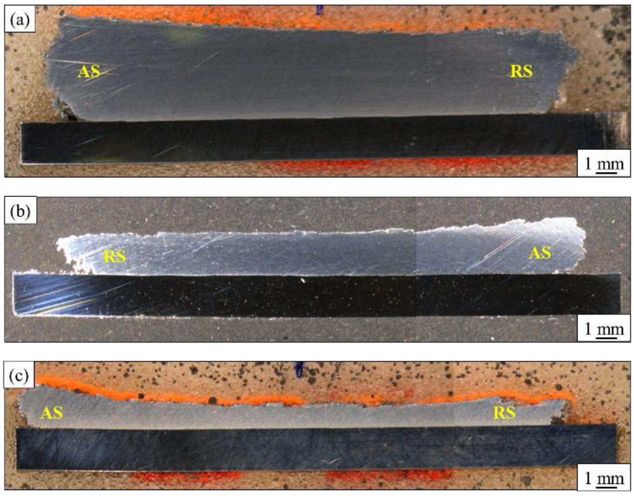

Fig. 4. Deposition morphology at different values of steel surface roughness R_a: (a) 1.5-2.5 µm (b) 5.5-6.5 µm (c) 7.5-8.5 µm

Table 3. Results of thickness measurement

Sr. No.	Substrate surface roughness, Ra, [µm]	Average coating thickness, [mm]
1.	1.5-2.5	3.52
2.	5.5-6.5	2.08
3.	7.5-8.5	1.115

As depicted in Fig. 4 (a), deposition thickness is higher on the advancing side (AS) compared to the retreating side (RS). Additionally, the centre region has the lowest thickness. Further, this effect is more significant for higher steel surface roughness (Figure 4 (c)). The width of the coating is slightly increased with an increase in the surface roughness.

As observed in Fig. 4 (a), (b) and (c), the average thickness of deposition decreases with an increase in the surface roughness of the steel substrate. The measured value of average thickness for different surface roughness is presented in Table 3. With an increase in surface roughness, more rubbing action occurs between consumable tool and steel substrate, resulting in higher heat generation and a reduction in deposition thickness. Kallien et al. [5] also concluded that the increase in process temperature leads to lower thickness and higher deposition width.

3.2. Deposition microstructure

In order to examine the microstructure of the as-deposited coating, the sample with R_a between (7.5-8.5)µm surface roughness is selected because this set of sample provides higher push-off strength compared to others.

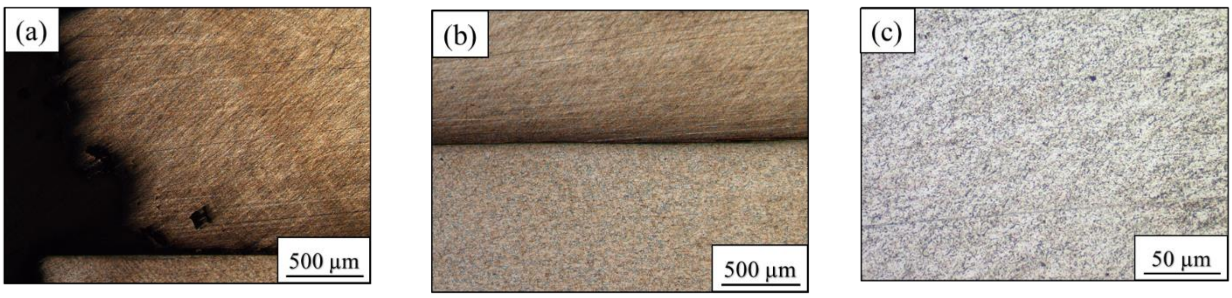

Fig. 5. Microstructure of friction surfacing deposition at the (a) edge (b) centre (c) coating region (Sample 3: 7.5-8.5 µm)

Fig. 5 shows the optical microscopy images obtained from the edge and centre region. As depicted in Fig. 5 (a) and (b), unbounded and undercut region is observed near the edge, whereas uniform microstructure without defects is observed at the centre. Additionally, signs of material flow from the Al-alloy rod with several cracks are also visible on the micrograph at the edge of the coating. Very fine Al grains are observed in the deposition microstructure, as presented in Fig. 5 (c). During deposition, grain refinement takes place in the coating region due to dynamic recrystallisation, resulting in fine-grain microstructure.

3.3. Interface characterisation

In order to understand the bonding mechanism between coating and substrate, interface characterisation is carried out by optical microscopy and SEM.

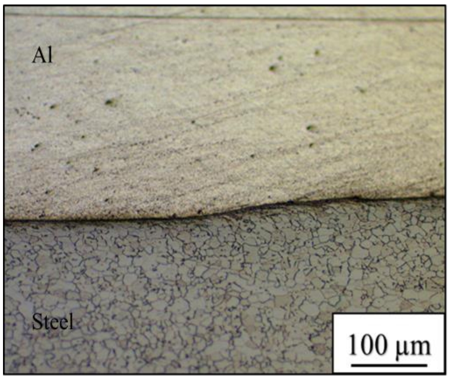

Fig. 6. Interface microstructure (Sample 3: 7.5-8.5 µm)

Fig. 6 shows the interface microstructure obtained by optical microscope for the sample with R_a =7.5-8.5 µm surface roughness. It is observed that plastic deformation takes place on the top region of the steel surface. As depicted in Fig. 6, compression and elongation along the faying interfaces is observed at the steel surface grains, representing that the process occurs in the solid state only.

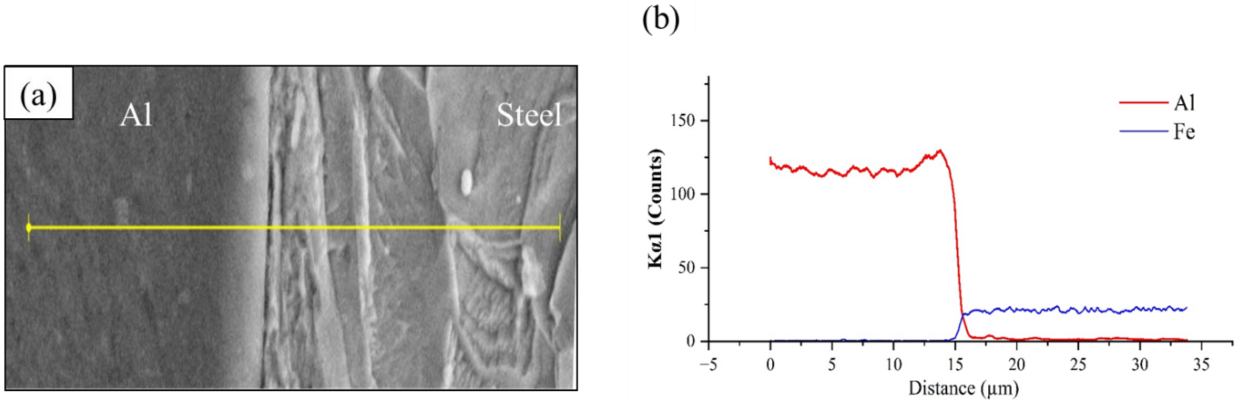

Fig. 7. (a) SEM micrograph at the interface (b) Results of EDS line scanning at the interface (Sample 3: R_a=7.5-8.5 µm)

The SEM micrograph of the interface is presented in Fig. 7 (a). It does not show any trace marks of intermetallic compound (IMC) formation at the interface. To elucidate about IMC formation, SEM-EDS line scanning is carried out on the yellow line marked in Fig. 7 (a). As depicted in Fig. 7 (b), the SEM-EDS line profile shows the continuous transition from Al to Fe instead of significant compositional changes at the interface. This reveals that IMC is not present at the interface. However, in-depth metallurgical analysis with advanced characterisation is required to provide a confirmed conclusion regarding the IMC formation at the interface.

3.4. Microhardness distribution

Microhardness analysis is carried out to understand the variation of mechanical properties due to heat generation during friction surfacing deposition. The hardness variation for the coating region, interface, steel substrate region as well as consumable tool are measured and presented in the bar graph, as shown in Fig. 8.

It is observed that Al is viscoelastically deformed and forms the deposition on a steel surface; hence, the microhardness of deposition is reduced to 66.57 HV from the consumable tool hardness of 101 HV. Moreover, hardness of the deposited layer remains uniform throughout the coating region as well as interface and features of strain hardening are not observed, indicating the recrystallisation of grains during the process.

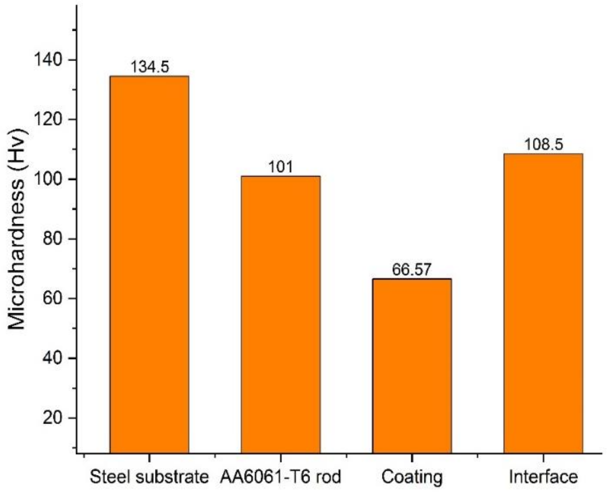

Fig. 8. Bar chart for microhardness (sample 3: Ra=7.5-8.5 μm)

3.5. Bonding strength and fractography

In order to determine the bonding strength of AA6061 and CR01, a push-off test is carried out. It has been observed that the substrate with R_a roughness values 1.5-2.5, 5.5-6.5 and 7.5-8.5 μm showed 26, 32 and 45 MPa push-off strength, respectively. The results showed that with an increase in the substrate surface roughness, the push-off strength increases. Higher surface roughness provides more asperities on the surface, which becomes as anchoring sites for mechanical interlocking and enhances the push-off strength.

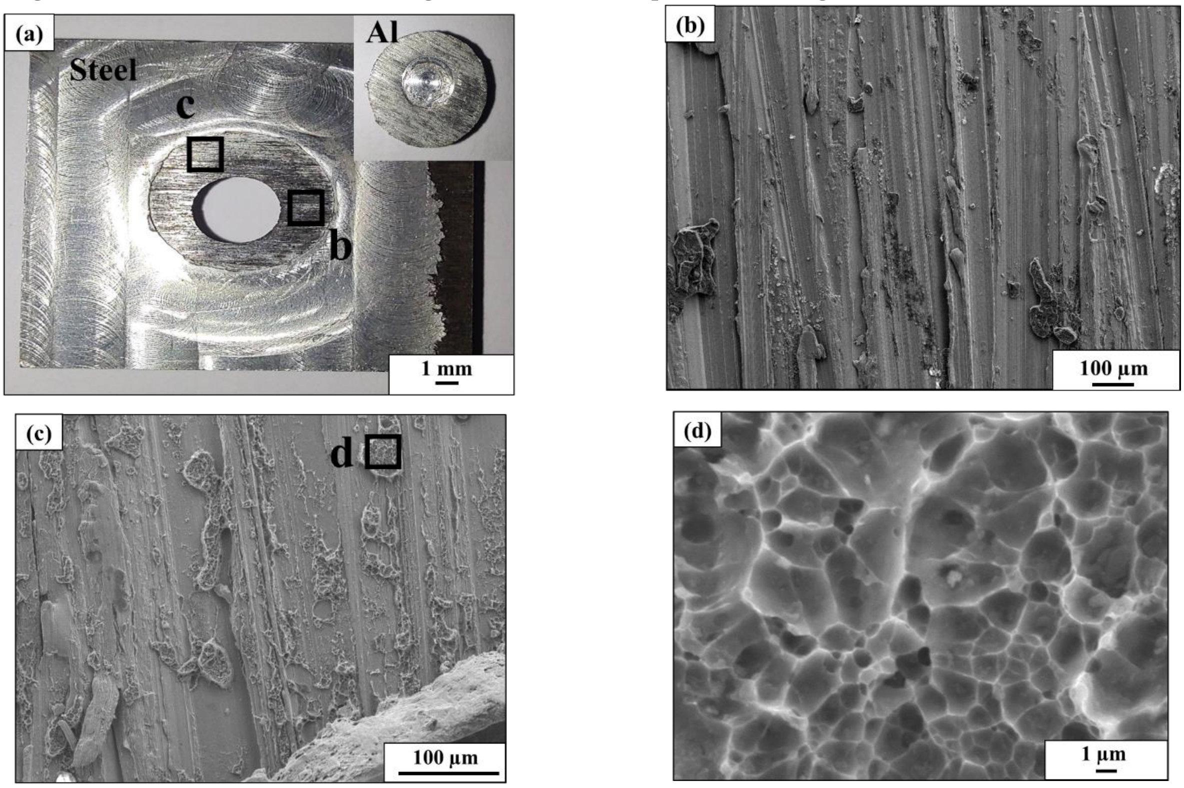

Fig. 9. SEM images of the fractured surface of push-off sample (Sample 3: R_a=7.5-8.5 μm)

All samples are failed from the interface. Sample with roughness value R_a=5.5-6.5 and R_a=7.5-8.5 show the sticking of some Al surface at the interface. To further analyse the failure type, fractography is carried out (using field-emission-scanning electron microscopy (FE-SEM) (Make: Jeol)), and higher magnification SEM images of the fracture surface are shown in Fig. 9. As shown in Fig. 9 (a) and (b), in the most of regions, failure is taken place from interface without any trace marks of Al on steel surface. However, at some regions, Al sticking is observed, as depicted in Fig. 9 (c). Fig. 9 (d) presents the higher magnification image for the location of Fig. 9 (c), and it represents dimples-like features at this region, indicating ductile failure of Al in this region.

4. CONCLUSIONS

In this article, the effect of substrate surface roughness on the push-off strength of the as-deposited AA6061-T6 coating on CR01 low-carbon steel is examined, along with its microstructural characterisation. The following conclusions have been drawn:

1. It is inferred from the test results that the push-off strength increases substantially with an increase in the substrate surface roughness. The higher surface roughness provides more asperities on the surface, which become as anchoring sites for mechanical interlocking and enhance the push-off strength. It is observed that the failure occurs from the interface in most regions without any trace marks of Al on the steel surface. However, in some regions, Al sticking is observed.
2. The macrostructural examination revealed that with an increase in substrate surface roughness, more rubbing action occurs between consumable tool and steel substrate, resulting in higher heat generation and reduction in deposition thickness.
3. During friction surfacing, grain refinement is observed at the coating region due to dynamic recrystallisation, which results in fine grain microstructure.

5. REFERENCES

1. Gandra, J., Krohn, H., Miranda, R. M., Vilaca, P., Quintino, L., Dos Santos, J. F., (2014). *Friction surfacing—A review*, J. Mater. Process. Tech., 214(5), 1062-1093.
2. Bedford, G. M., Vitanov, V. I., Voutchkov, I. I., (2001). *On the thermo-mechanical events during friction surfacing of high speed steels*, Surf. Coat. Technol., 141(1), 34-39.
3. Seidi, E., Miller, S. F., Carlson, B. E., (2021). *Friction surfacing deposition by consumable tools*, J. Manuf. Sci. Eng., 143(12), pp. 120801.
4. Kumar, B.V., Reddy, G.M. and Mohandas, T., (2015). *Influence of process parameters on physical dimensions of AA6063 aluminium alloy coating on mild steel in friction surfacing.* Def. Technol., 11(3), 275-281.
5. Kallien, Z., Rath, L., Roos, A., Klusemann, B., (2020). *Experimentally established correlation of friction surfacing process temperature and deposit geometry*, Surf. Coat. Technol., 397, pp. 126040.
6. Vitanov, V.I., Javaid, N. and Stephenson, D.J., (2010). *Application of response surface methodology for the optimisation of micro friction surfacing process.* Surf. Coat. Technol., 204(21-22), 3501-3508.
7. Galvis, J.C., Oliveira, P.H.F., Hupalo, M.F., Martins, J.P. and Carvalho, A.L.M., (2017). *Influence of friction surfacing process parameters to deposit AA6351-T6 over AA5052-H32 using conventional milling machine.* J. Mater. Process. Technol., 245, 91-105.
8. Da Silva, M. M., Afonso, M. L. B., Silva, S. L. N., Troysi, F. C. T. D., dos Santos, I. B., Brito, P.P., (2018). *Application of the friction surfacing process in a CNC machining center: a viability assessment for producing Al-alloy coatings on low carbon steel*, J. Braz. Soc. Mech. Sci., 40, 1-11.
9. Troysi F., Santos, I. B., Silva, K., Brito, P., (2016). *Analysis of the friction surfacing process applied in a CNC machining center for deposition of austenitic stainless steel on carbon steel substrates*. Proceedings of the 9th National Congress of Mechanical Engineering (IX CONEM), Vol. 1, Rio de Janeiro, Brazil.
10. Troysi, F., Silva, K., Santos, I. D., Brito, P., (2019). *Investigation of austenitic stainless steel coatings on mild steel produced by friction surfacing using a conventional CNC machining center*, Mater. Res., 22, pp. e20180301.
11. Lu, Y., Mayton, E., Song, H., Kimchi, M., Zhang, W., (2019). *Dissimilar metal joining of aluminum to steel by ultrasonic plus resistance spot welding-microstructure and mechanical properties*, Mater. Design, 165, pp. 107585.

Received: April 01, 2023 / Accepted: December 15, 2023 / Paper available online: December 20, 2023 © International Journal of Modern Manufacturing Technologies